

reasonable description of the likely interactions between DDP and DNA.

The primary aim of the present study was to investigate stereochemical explanations for the observation that DDP binds to ApG but not GpA sequences of DNA. It has been predicted on the basis of an idealized model of DNA that this dichotomy is the result of differences in the distance from a Pt atom bound monofunctionally to N7 of adjacent bases in the 3'- and 5'-directions.<sup>8</sup> We have modeled a number of monofunctional interactions in order to investigate this suggestion further. Our initial, idealized, models do show the difference in the distances to the 3'- and 5'-bases as proposed previously, but these differences disappear or are reversed on energy minimization. This is primarily the result of rotation of the plane of the purine base following monofunctional complexation, and in general the distances to the 3'- and 5'-bases are similar. Thus, our models do not provide support for the suggestion that differences in the distances to the 3'- and 5'-bases are responsible for the nonoccurrence of DDP binding to GpA sequences of DNA.

Since the monofunctional adducts do not appear to offer an explanation, we have modeled both the formation and the structure of the bifunctional adducts. Transition-state and ground-state models of bifunctional adducts with ApG and GpA sequences

reveal significant differences. In the ApG adducts, there is an H-bond between an ammine ligand and O6 of the 3'-guanine, and in the GpA adducts, there is a repulsive contact between the equivalent ammine ligand and the -NH<sub>2</sub> of the 3'-adenine. We propose that the latter interaction destabilizes the transition state sufficiently to prevent formation of the DDP-GpA adduct.

The proposal that interactions between an ammine ligand and groups in the 6-position of the 3'-purine influence binding specificity might be tested by designing a compound able to interact favorably with the -NH<sub>2</sub> groups of adenine. Such a compound should be able to bind to GpA sequences. Recent molecular modeling suggests that a complex with one amine donor group and one sulfoxide donor group would be ideal stereochemically. We have prepared a number of these compounds and are currently studying their interaction with DNA.

**Acknowledgment.** We wish to acknowledge the support of the Sydney University Cancer Research Fund and use of the Sydney University Biomolecular Graphics Facility.

**Supplementary Material Available:** A listing of force field parameters and a chart showing the atom identifiers (6 pages). Ordering information is given on any current masthead page.

Contribution from the Department of Chemistry, University of Newcastle, New South Wales 2308, Australia, Institut für Anorganische Chemie, Universität Basel, 4056 Basel, Switzerland, and School of Chemistry, University of Sydney, New South Wales 2006, Australia

## Coordination of the Sexidentate Macrocyclic

### 6,13-Dimethyl-1,4,8,11-tetraazacyclotetradecane-6,13-diamine to Iron(III)

Paul V. Bernhardt,<sup>1</sup> Peter Comba,<sup>2</sup> Trevor W. Hambley,<sup>3</sup> and Geoffrey A. Lawrance\*<sup>1</sup>

Received July 20, 1990

The sexidentate polyamine macrocycle 6,13-dimethyl-1,4,8,11-tetraazacyclotetradecane-6,13-diamine (diammac) reacts with iron(II) in aqueous solution to form the low-spin iron(III) complex Fe(diammac)<sup>3+</sup>. Crystals of [Fe(diammac)](ClO<sub>4</sub>)Cl<sub>2</sub> are monoclinic, space group *C*<sub>2</sub>/*c*, with *a* = 15.6612 (8) Å, *b* = 7.4390 (7) Å, *c* = 18.061 (2) Å, and β = 108.626 (7)°. The Fe(diammac)<sup>3+</sup> ion is stable indefinitely in aerated aqueous solution, and its electronic and electron paramagnetic resonance spectra are consistent with a low-spin d<sup>5</sup> electronic ground state. In aqueous base, deprotonation (p*K*<sub>a</sub> 10.2 ± 0.2) is accompanied by a color change to red, but the deprotonated species is not stable. The reversible Fe<sup>III/II</sup> redox couple occurs at a quite negative potential (-0.35 V vs Ag/AgCl; Δ*E* = 60 mV at 10-500 mV/s scan rate for cyclic voltammetry at glassy carbon) compared with other iron(III) complexes. Although the couple is reversible on the voltammetric time scale, monitoring the chemical reduction with zinc amalgam by NMR spectroscopy showed metal ion exchange occurs. Detailed analysis of the EPR and electronic spectra was possible; from the latter, along with comparisons with five other octahedral complexes of diammac, the empirical ligand spectroscopic parameter, *g*, for Fe(III) has been reassessed as 16.3 cm<sup>-1</sup>, and sexidentate diammac has been defined as the strongest purely σ-bonded ligand extant.

## Introduction

The nitrogen-donor coordination chemistry of iron(III) is dominated by complexes containing strong π-acceptor ligands such as porphyrins and bipyridine. In stark contrast, there have been very few reports of (hexaamine)iron(III) complexes in the literature.<sup>4-6</sup> Moreover, these complexes have in some cases been stable for extended periods only in the solid state, although the recent chemistry of (tacn)<sub>2</sub> complexes (tacn = 1,4,7-triazacyclononane)<sup>5,6</sup> indicates that solution-stable hexaamines can be accessible. As a consequence of the limited examples of (hexaamine)iron(III) compounds, the interesting spectroscopic and electrochemical properties of these complexes have remained relatively unexplored.

Hexaamine complexes are ideal for studying the electronic properties of metal complexes in strong ligand fields free from charge-transfer transitions, but only one assignment of the electronic spectrum of a (hexaamine)iron(III) complex has appeared in the literature. This comprised a report of the solid-state, diffuse-reflectance spectrum of tris(ethylenediamine)iron(III) chloride, which is not stable in aqueous solution.<sup>4</sup> Also, the low-spin d<sup>5</sup> electronic configuration typical of (hexaamine)iron(III) complexes is particularly amenable to analysis by electron paramagnetic resonance (EPR) spectroscopy without the complications of electron delocalization.

As a continuation of our studies of the coordination chemistry of the strong ligand field, pendant-arm macrocycle 6,13-dimethyl-1,4,8,11-tetraazacyclotetradecane-6,13-diamine (diammac),<sup>7-11</sup> we have investigated its complexation of iron(III). A

(1) University of Newcastle.

(2) Universität Basel.

(3) University of Sydney.

(4) Renovitch, G. A.; Baker, W. A., Jr. *J. Am. Chem. Soc.* **1968**, *90*, 3583.

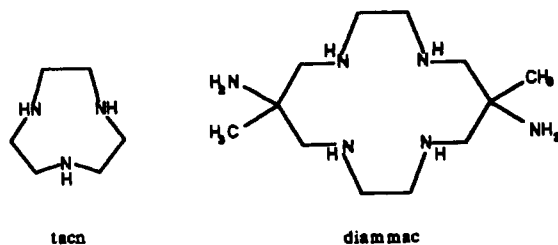
(5) Wiegardt, K.; Schmidt, W.; Herrmann, W.; Küppers, H.-J. *Inorg. Chem.* **1983**, *22*, 2953.

(6) Wiegardt, K.; Tolksdorf, I.; Herrmann, W. *Inorg. Chem.* **1985**, *24*, 1230.

(7) Bernhardt, P. V.; Lawrance, G. A.; Hambley, T. W. *J. Chem. Soc., Dalton Trans.* **1989**, 1059.

(8) Bernhardt, P. V.; Lawrance, G. A.; Hambley, T. W. *Aust. J. Chem.* **1990**, *43*, 699.

(9) Bernhardt, P. V.; Comba, P.; Curtis, N. F.; Hambley, T. W.; Lawrance, G. A.; Maeder, M.; Siriwardena, A. *Inorg. Chem.* **1990**, *29*, 3208.



preliminary report of this work has been communicated.<sup>12</sup> Herein, we report the synthesis, physical properties, and X-ray crystal structure of a low-spin iron(III) complex of diammac.

### Experimental Section

**Synthesis.** (6,13-Dimethyl-1,4,8,11-tetraazacyclotetradecane-6,13-diamine)iron(III) Perchlorate Hydrate,  $[\text{Fe}(\text{diammac})](\text{ClO}_4)_3 \cdot \text{H}_2\text{O}$ . The preparation of diammac-6HCl has been described previously.<sup>7</sup> A solution of iron(II) sulfate heptahydrate (0.54 g) in water (100 mL) was purged with nitrogen for 15 min. With the nitrogen supply continued, a deoxygenated solution of diammac-6HCl (1.0 g) in water (40 mL), previously neutralized with dilute sodium hydroxide, was added dropwise over 1 h. The nitrogen supply was discontinued, the vessel sealed, and the solution stirred at room temperature for 24 h. The solution was exposed to the atmosphere, diluted to 0.5 L, and sorbed on a column of SP-Sephadex C-25 cation-exchange resin ( $\text{Na}^+$  form). Washing with 0.2 M  $\text{NaClO}_4$  removed uncomplexed species, and the desired product was removed with 0.5 M  $\text{NaClO}_4$  and concentrated to ca. 100 mL on a rotary evaporator. Upon standing for 24 h, yellow crystals of the product formed and were collected, washed with ethanol and then diethyl ether, and dried in a vacuum desiccator (0.65 g, 55%). Anal. Calcd for  $\text{C}_{12}\text{H}_{30}\text{Cl}_3\text{FeN}_6\text{O}_{13}$ : C, 22.85; H, 5.1; N, 13.3. Found: C, 23.1; H, 5.1; N, 13.3. Slow evaporation of a solution of  $[\text{Fe}(\text{diammac})](\text{ClO}_4)_3$  (0.1 g) and sodium chloride (0.1 g) in water (20 mL) afforded yellow crystals of the mixed salt suitable for X-ray analysis.

**Physical Methods.** Electronic spectra were measured on Hitachi 150-20 UV-vis and Cary 2300 UV-vis-near-IR spectrophotometers. Infrared spectra were measured on a Nicolet MX-1 FT-IR spectrometer with samples being dispersed in KBr disks. Electron paramagnetic resonance (EPR) spectra were recorded on a Varian E9 spectrometer ( $\nu = 8.926$  GHz) as ca.  $10^{-3}$  M solutions of complex in DMF/ $\text{H}_2\text{O}$  (1:2) at 77 K. Cyclic voltammetry was performed with a BAS CV-27 controller employing a glassy-carbon working electrode, a silver/silver chloride reference electrode, and a platinum counter electrode. Polarography was performed with an AMEL Model 457 controller and a PAR Model 303 dropping-mercury working electrode, with other electrodes as described above. All aqueous solutions were 0.1 M in  $\text{NaClO}_4$  and were purged with nitrogen. The magnetic moment of  $[\text{Fe}(\text{diammac})](\text{ClO}_4)_3$  at 295 K was determined by the Evans NMR method,<sup>13</sup> with measurements being made with a JEOL FX90Q FT-NMR spectrometer. The solvent system was 2% 2-methylpropan-2-ol in  $\text{D}_2\text{O}$ , with the shift in the  $^1\text{H}$  resonance of the methyl groups being used to calculate the magnetic moment.

**Structure Analysis.** For the structure of  $[\text{Fe}(\text{diammac})](\text{ClO}_4)_2\text{Cl}_2$ , lattice dimensions were determined by a least-squares fit to the setting parameters of 25 independent reflections, measured and refined on an Enraf-Nonius CAD4 four-circle diffractometer employing graphite-monochromated  $\text{Mo K}\alpha$  radiation. Crystallographic data are summarized in Table I. Data reduction and application of Lorentz, polarization, and decomposition corrections were carried out by using the Enraf-Nonius Structure Determination Package.<sup>14</sup>

The structure was solved by heavy-atom methods and refined by full-matrix least-squares analysis with SHELX-76.<sup>15</sup> All non-hydrogen atoms with the exception of minor sites of C (ligand) and O (perchlorate) atom disorder were refined anisotropically. For hydrogen atoms positional parameters and an isotropic thermal parameter were refined. Scattering factors and anomalous dispersion corrections for Fe were taken

Table I. Crystal Data for  $[\text{Fe}(\text{diammac})](\text{ClO}_4)_2\text{Cl}_2$

space group	$C2/c$	empirical formula	$\text{C}_{12}\text{H}_{30}\text{Cl}_3\text{FeN}_6\text{O}_4$
$a$ , Å	15.6112 (8)	$Z$	4
$b$ , Å	7.4390 (7)	abs coeff, $\text{cm}^{-1}$	11.92
$c$ , Å	18.061 (2)	transm coeffs	0.723–0.918
$\beta$ , deg	108.626 (7)	temp, °C	21
$V$ , Å <sup>3</sup>	1994 (1)	$\lambda$ , Å	0.71069
fw	484.62	$R(F_o)^a$	0.025
$D_c$ , $\text{g cm}^{-3}$	1.616	$R_w(F_o)^b$	0.029

$$^a R(F_o) = \sum(|F_o| - |F_c|) / \sum(|F_o|). \quad ^b R_w(F_o) = (\sum w(|F_o| - |F_c|)^2 / \sum w(|F_o|)^2)^{1/2}; w = 3.77 / (\sigma^2 |F_o| + (7.8 \times 10^{-5}) |F_o|^2).$$

Table II. Positional Parameters ( $\times 10^4$ ) for  $[\text{Fe}(\text{diammac})](\text{ClO}_4)_2\text{Cl}_2$

	$x$	$y$	$z$	occupancy
Fe(1)	0	0	0	0.5
N(1)	1123 (1)	378 (2)	-53 (1)	
N(2)	-221 (1)	-1571 (2)	-922 (1)	
N(3)	-661 (1)	1800 (2)	-804 (1)	
C(1)	-1888 (2)	260 (3)	-678 (2)	
C(2)	-1414 (1)	747 (3)	-1269 (1)	
C(3)	-1008 (2)	-881 (3)	-1551 (1)	
C(4)	655 (2)	-1859 (5)	-1066 (2)	0.78 (1)
C(5)	1242 (2)	-272 (5)	-824 (2)	0.78 (1)
C(4')	-498 (7)	1123 (19)	1322 (7)	0.22 (1)
C(5')	-1404 (7)	1161 (16)	580 (6)	0.22 (1)
C(6)	-2048 (2)	1781 (3)	-1954 (2)	
Cl(1)	0	5833 (1)	2500	0.5
O(1)	-624 (2)	4803 (3)	2721 (2)	0.90 (1)
O(2)	-629 (6)	6184 (11)	1656 (3)	0.45 (1)
O(3)	-138 (6)	7572 (7)	2228 (3)	0.45 (1)
O(4)	440 (21)	6925 (41)	3086 (20)	0.10 (2)
O(5)	282 (17)	5393 (31)	1888 (13)	0.10 (2)
O(6)	-966 (17)	5242 (24)	2101 (16)	0.10 (2)
Cl(2)	1392 (1)	5488 (1)	5338 (1)	

from ref 16, while all others were supplied in SHELX-76 and plots were drawn by using ORTEP.<sup>17</sup> Non-hydrogen atom coordinates are listed in Table II. Listings of H atom coordinates, anisotropic thermal parameters, close intermolecular contacts, and observed and calculated structure factor amplitudes have been deposited as supplementary material.

### Results and Discussion

Reaction of ferrous sulfate with diammac in aqueous solution initially under a nitrogen atmosphere generates the  $[\text{Fe}(\text{diammac})]^{3+}$  cation in reasonable yield. The reaction does proceed under aerobic conditions but with a diminished yield. The facile and rapid oxidation of ferrous solutions in aerobic, basic conditions to ferric hydrated oxides is the most likely cause of the poorer yield in the latter case. The complex, unlike most known (hexaamine)iron(III) complexes, is indefinitely stable in aerated neutral aqueous solution. The complex displays an amine deprotonation process characterized by a red color ( $\lambda_{\text{max}}$  ca. 500 nm) in aqueous base, with a  $\text{pK}_a$  defined by a spectrophotometric titration of  $10.2 \pm 0.2$ . The complex is not stable above pH 10, and the red color of the solution fades relatively rapidly to yield a brown precipitate of apparently ferric hydroxide. The behavior in aqueous base is similar to that reported for  $[\text{Fe}(\text{tacn})_2]^{3+}$ , where a deprotonation with a  $\text{pK}_a$  of  $11.4 \pm 0.4$  has been defined, although the process in that case was reversible on the addition of acid, the deprotonated species being more stable.<sup>18</sup> The lower  $\text{pK}_a$  in the case of diammac may be related to the shorter Fe–N bonds and consequently greater inductive effects, although comparisons of different ligands are tenuous at best.

Electrochemistry of  $[\text{Fe}(\text{diammac})]^{3+}$  found the  $\text{Fe}^{\text{III/II}}$  couple at  $E_{1/2} = -0.35$  V versus Ag/AgCl. This value is one of the most negative potentials reported for an iron complex of any description but especially negative for a (hexaamine)iron(III) complex. The couple is totally reversible on the voltammetric time scale, as

- Bernhardt, P. V.; Lawrance, G. A.; Hambley, T. W. *J. Chem. Soc., Dalton Trans.* 1990, 983.
- Bernhardt, P. V.; Lawrance, G. A.; Skelton, B. W.; White, A. H. *Aust. J. Chem.* 1989, 42, 1035.
- Bernhardt, P. V.; Hambley, T. W.; Lawrance, G. A. *J. Chem. Soc., Chem. Commun.* 1989, 553.
- Löfliger, J.; Scheffold, R. *J. Chem. Educ.* 1972, 49, 646.
- Enraf-Nonius Structure Determination Package (SDP); Enraf-Nonius: Delft, Holland, 1985.
- Sheldrick, G. M. *SHELX-76, A Program for X-ray Crystal Structure Determination*; University of Cambridge: Cambridge, U.K., 1976.

- Cromer, D. T.; Waber, J. T. *International Tables for X-ray Crystallography*; Kynoch Press: Birmingham, U.K., 1974; Vol. IV.
- Johnson, C. K. *ORTEP, A Thermal Ellipsoid Plotting Program*; Oak Ridge National Laboratory: Oak Ridge, TN, 1965.
- Pohl, K.; Wieghardt, K.; Kaim, W.; Steenzen, S. *Inorg. Chem.* 1988, 27, 440.

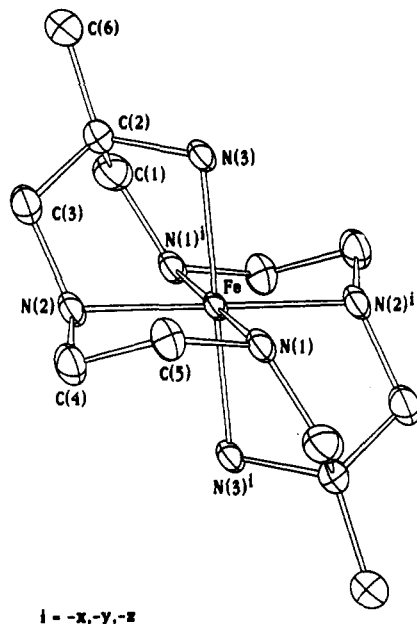
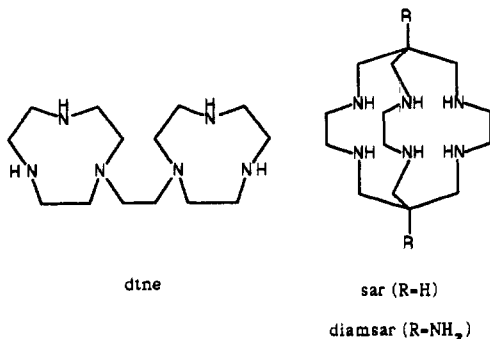


**Figure 1.** ORTEP drawing  $[\text{Fe}(\text{diammac})]^{3+}$ , showing the crystallographic numbering. Probability ellipsoids of 30% are shown (hydrogen atoms omitted).

indicated by cyclic voltammetry ( $\Delta E = 60$  mV;  $i_{pc}/i_{pa} = 1.0$ ), where the separations of the anodic and cathodic peak potentials were independent of scan rate in the range 10–500  $\text{mV s}^{-1}$ .

Attempts to isolate the iron(II) complex of diammac following reduction were basically unsuccessful. Chemical reduction of  $[\text{Fe}(\text{diammac})]^{3+}$  with zinc amalgam under a nitrogen atmosphere at 60 °C generated a transient green solution with electronic maxima at 17 065, and 24 631  $\text{cm}^{-1}$ , characteristic of a low-spin iron(II) hexaamine and comparable with the spectrum of the hexaamine  $\text{Fe}(\text{diansar})^{2+}$  (17 007 and 25 000  $\text{cm}^{-1}$ ).<sup>19</sup>



The green color of the solution faded within minutes on heating, even in anaerobic conditions, to give a colorless solution with a  $^1\text{H}$  NMR spectrum identical with that of  $\text{Zn}(\text{diammac})^{2+}$ , the (hexaamine)zinc(II) complex having been prepared via another route.<sup>20</sup> Even near room temperature, following the reaction in situ by  $^1\text{H}$  NMR spectroscopy showed relatively rapid metal ion exchange, indicative of a modest stability constant for the iron(II) complex of diammac. Reduction of  $[\text{Fe}(\text{diammac})]^{3+}$  with zinc amalgam in dilute acid followed by crystallization with dithionato led to isolation of only the *trans*- $[\text{Zn}(\text{diammacH}_2)(\text{S}_2\text{O}_6)_2]$  complex where the pendant amines were found to be protonated with the dithionato ligands coordinating in the axial sites of the complex.<sup>8</sup>

The structure of  $[\text{Fe}(\text{diammac})]^{3+}$  as the triperchlorate salt has been communicated,<sup>12</sup> whereas the structure of the mixed chloride perchlorate salt is reported here. The structure of  $[\text{Fe}(\text{diam-$

**Table III.** Bond Lengths (Å) for  $[\text{Fe}(\text{diammac})](\text{ClO}_4)_2$ <sup>a</sup>

N(1)–Fe(1)	1.969 (2)	N(2)–Fe(1)	1.974 (2)
N(3)–Fe(1)	1.984 (2)	C(5)–N(1)	1.484 (3)
C(3)–N(2)	1.477 (3)	C(4)–N(2)	1.493 (3)
C(2)–N(3)	1.492 (2)	C(4')–N(2)	1.556 (9)
C(5')–N(1)	1.571 (9)	C(2)–C(1)	1.525 (3)
C(3)–C(2)	1.530 (3)	C(6)–C(2)	1.524 (3)
C(5)–C(4)	1.474 (5)	C(5')–C(4')	1.611 (17)
C(1)–N(1) <sup>i</sup>	1.478 (3)	O(1)–Cl(1)	1.397 (2)
O(2)–Cl(1)	1.550 (6)	O(3)–Cl(1)	1.376 (5)
O(4)–Cl(1)	1.337 (36)	O(5)–Cl(1)	1.355 (22)
O(6)–Cl(1)	1.520 (25)		

<sup>a</sup>i indicates symmetry coordinates  $-x, -y, -z$ .

**Table IV.** Bond Angles (deg) for the  $[\text{Fe}(\text{diammac})]^{3+}$  Cation<sup>a</sup>

N(2)–Fe(1)–N(1)	87.4 (1)	N(3)–Fe(1)–N(1)	96.8 (1)
N(3)–Fe(1)–N(2)	82.4 (1)	C(5)–N(1)–Fe(1)	108.1 (1)
N(1)–Fe(1)–N(1) <sup>i</sup>	180.0	C(3)–N(2)–Fe(1)	108.8 (1)
C(4)–N(2)–Fe(1)	108.0 (1)	C(4)–N(2)–C(3)	120.3 (2)
N(2)–Fe(1)–N(2) <sup>i</sup>	180.0	C(2)–N(3)–Fe(1)	100.4 (1)
N(3)–Fe(1)–N(3) <sup>i</sup>	180.0	C(1)–C(2)–N(3)	104.0 (2)
C(3)–C(2)–N(3)	103.8 (2)	C(3)–C(2)–C(1)	113.1 (2)
C(6)–C(2)–N(3)	113.9 (2)	C(6)–C(2)–C(1)	110.6 (2)
C(6)–C(2)–C(3)	111.1 (2)	C(2)–C(3)–N(2)	110.6 (2)
C(5)–C(4)–N(2)	110.7 (2)	C(4)–C(5)–N(1)	110.0 (3)
C(5)–N(1)–C(1) <sup>i</sup>	121.0 (2)		

<sup>a</sup>i indicates symmetry coordinates  $-x, -y, -z$ .

**Table V.** Physical Properties of (Hexaamine)iron(III) Complexes

ligand	$\nu$ , $\text{cm}^{-1}$	$E_{1/2}$ , V <sup>a</sup>	Fe–N, Å	ref
diammac	20 833 23 981 30 120	–0.35	1.969–1.984	this work
sar <sup>b</sup>	18 904 22 831 27 322	–0.15	2.01	21
dtne <sup>c</sup>	21 882 28 169	+0.19	1.980–2.021	6, 22
(tacn) <sub>2</sub>	20 000 23 256 29 762	–0.09	1.998	5, 23
(en) <sub>3</sub>	18 500 21 500 27 500			4

<sup>a</sup>Vs Ag/AgCl. <sup>b</sup>sar = 3,6,10,13,16,19-hexaazabicyclo[6.6.6]eicosane. <sup>c</sup>dtne = 1,2-bis(1,4,7-triaza-1-cyclononyl)ethane.

mac)]( $\text{ClO}_4$ )<sub>3</sub> exhibited a high degree of disorder in the perchlorate oxygen atoms, and the precision of the structure suffered as a consequence. The mixed chloride perchlorate salt of  $[\text{Fe}(\text{diammac})]^{3+}$  afforded crystals of superior quality to those employed in the triperchlorate structure. Moreover, perchlorate disorder was obviously not a dominant feature in the present structure, and a more precise refinement was achieved. Nevertheless, the geometries of the complex cations in the triperchlorate and dichloride perchlorate structures were not significantly different. The perchlorate dichloride salt is isostructural with the cobalt(III) complex of diammac<sup>7</sup> and comprises the complex cation on a center of symmetry, a chloride anion on a general site, and a perchlorate anion sited on a 2-fold rotation axis. An ORTEP<sup>17</sup> drawing of  $[\text{Fe}(\text{diammac})]^{3+}$  is given in Figure 1, with bond lengths and angles appearing in Tables III and IV, respectively. Sexidentate coordination of diammac to the iron center is apparent with the macrocycle encircling the metal ion and the pendant primary amines coordinating in the axial sites above and below the macrocyclic plane. All C–C and C–N bond lengths were in the range 1.47–1.53 Å, indicative of single bonds. The equatorial Fe–N(macrocycle) bond lengths (average 1.972 Å) are somewhat shorter than the axial Fe–N(pendant) bonds (average 1.984 Å), although both sets are particularly short for an iron(III) hexaamine<sup>21–23</sup> (Table V).

(19) Martin, L. L.; Hagen, K. S.; Hauser, A.; Martin, R. L.; Sargeson, A. M. *J. Chem. Soc., Chem. Commun.* **1988**, 1313.

(20) Bernhardt, P. V.; Lawrence, G. A.; Maeder, M.; Rossignoli, M.; Hambley, T. W. *J. Chem. Soc., Dalton Trans.*, in press.

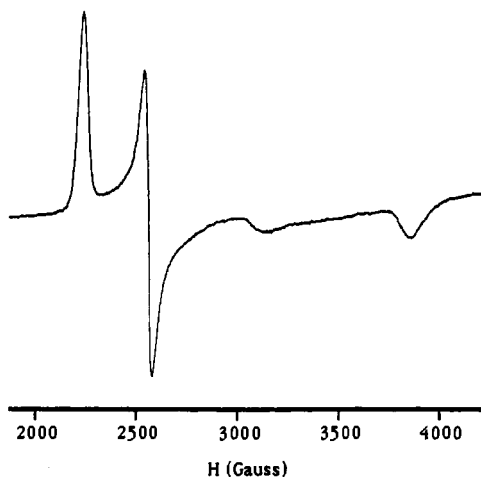


Figure 2. EPR spectrum of  $[\text{Fe}(\text{diammac})]^{3+}$  at 77 K. The broad peak at ca. 3200 G is due to a contaminant in the probe.

Unusually short M–N bond lengths have now been observed in  $\text{Fe}(\text{III})$ ,  $\text{Co}(\text{III})$ ,<sup>7</sup>  $\text{Cr}(\text{III})$ ,<sup>9</sup>  $\text{Rh}(\text{III})$ ,<sup>10</sup>  $\text{Ni}(\text{II})$ ,<sup>24</sup> and  $\text{Zn}(\text{II})$ <sup>20</sup> complexes of diammac where the ligand, in each case, acts as a sexidentate one. Molecular mechanics calculations on  $\text{Co}(\text{diammac})^{3+}$  showed that the exceptionally short Co–N bond lengths were a result of ligand demands.<sup>25</sup> In other words, a minimization of intraligand strain leads to a relatively small deviation of the Co–N bonds from anticipated “strain-free” distances (ca. 1.925 Å). The metal–nitrogen distances in the present structure similar to those in the isostructural cobalt(III) complex allow an argument along the same lines to explain the short Fe–N bond lengths found in  $\text{Fe}(\text{diammac})^{3+}$ , although electronic effects may also influence the outcome. For example, in the  ${}^2T_{2g}$  ground electronic state found in  $\text{Fe}(\text{diammac})^{3+}$  a Jahn–Teller distortion of the octahedral coordination sphere is expected to operate so steric arguments alone would, on the surface, appear to be inadequate when the observed Fe–N distances are explained. On the other hand, the observed axial elongation of the Fe–N bond lengths in the present structure cannot only be attributed to electronic effects since, similar distortions have been observed in each of the remaining five M(diammac)<sup>n+</sup> structures, and in those cases Jahn–Teller distortions were not operative. Importantly, when less than six of the amine donors are coordinated in complexes of diammac, the M–N bond lengths are not particularly unusual,<sup>24</sup> so comparisons of sexidentate diammac complexes with other hexaamines should only be made here.

Coordination of the macrocycle has previously been observed to result in large deformations in the ligand, and this is observed in the present structure. Most notable are the Fe–N(3)–C(2) angles [100.4 (1)°] and the N(3)–C(2)–C(1, 3) angles [103.8 (2) and 104.0 (2)°]. The ethylenediamine links in the ligand are disordered between the  $\delta$  and  $\lambda$  conformers, as has been observed previously in related structures of  $[\text{M}(\text{diammac})](\text{ClO}_4)_3$  (M = Cr, Rh, and Fe).<sup>9,10,12</sup> In those structures the disorder was manifested in large thermal parameters for the C atoms in the five-membered chelate rings, but in the present structure we have been able to resolve the disorder and refine major and minor sites for these atoms. The perchlorate anion is rotationally disordered over a number of sites.

The anisotropic EPR spectrum of  $\text{Fe}(\text{diammac})^{3+}$  at 77 K is shown in Figure 2. The spectrum is consistent with a low-spin  $d^5$  complex in a distorted octahedral ligand field with three resonances at  $g$  values of 2.841, 2.463, and 1.631 being observed.

No spectrum was observed at 295 K, a result of a short spin–lattice relaxation time common to low-spin  $d^5$  complexes.<sup>26</sup> The interpretation of EPR spectra of low-spin iron(III) complexes is less complicated when one can assume little or no delocalization of the  $t_{2g}$  electrons onto the ligand; i.e., the  $t_{2g}$  orbitals can be assumed to be essentially of metal character. This assumption is valid in the case of  $\text{Fe}(\text{diammac})^{3+}$ , where the Fe–N bonds can be considered as virtually pure  $\sigma$  bonds. The relevant theory used in the interpretation of the EPR spectrum of a low-spin  $d^5$  complex is described elsewhere,<sup>27</sup> but a brief description is appropriate here. The  ${}^2T_{2g}$  electronic ground state is 6-fold degenerate when spin is included. The action of spin–orbit coupling and lower than octahedral symmetry lifts this degeneracy, and three Kramer's doublets result, with resonance being observed within the lowest energy doublet. The components of this lowest energy doublet may be described by linear combinations of the  $t_{2g}$  basis functions

$$|+\rangle = A|1+\rangle + \frac{1}{2}B[\sqrt{2}(|2-\rangle - |-2-\rangle)] + C|-1+\rangle \quad (1)$$

$$|-\rangle = -A|-1-\rangle + \frac{1}{2}B[\sqrt{2}(|2+\rangle - |-2+\rangle)] - C|-1-\rangle \quad (2)$$

where

$$A^2 + B^2 + C^2 = 1 \quad (3)$$

It may be shown that the observed  $g$  values are related to the coefficients  $A$ ,  $B$ , and  $C$  by

$$A = (g_x + g_y - 2g_z)/4(g_x + g_y - g_z)^{1/2} \quad (4)$$

$$B = (g_y + g_x)/2(2(g_x + g_y - g_z))^{1/2} \quad (5)$$

$$C = (g_y - g_x)/4(g_x + g_y - g_z)^{1/2} \quad (6)$$

and these coefficients are related to the axial distortion,  $\mu$ , and rhombic distortion parameters,  $R$ , the energy of the Kramer's doublet,  $E_1$ , and the spin–orbit coupling constant,  $\lambda$ , by

$$\mu/\lambda = [-A^2 + B^2 + C^2 + (AB + BC^2/A)/\sqrt{2}]/\sqrt{2}(-AB + BC^2/A) \quad (7)$$

$$R/\lambda = (2AC + \sqrt{2}BC)/(C^2 - A^2) \quad (8)$$

$$E_1/\lambda = \frac{2}{3}(\mu/\lambda) - (A/\sqrt{2}B) \quad (9)$$

Therefore, the observed  $g$  values may be related to the parameters that describe the electronic ground state of the complex. The problem then is to assign the three  $g$  values to  $g_x$ ,  $g_y$ , and  $g_z$  and to determine the sign of each one as the experiment yields only the magnitude. By substitution of all 48 combinations of the three  $g$  values (both positive and negative) into (4)–(6), there are only six combinations that satisfy the normalization condition (eq 3). From these six, there is then but one combination that satisfies the conditions that  $|\mu/\lambda|$  is a maximum and that  $R/\lambda$  is positive, namely

$$g_x = 2.841 \quad g_y = 2.463 \quad g_z = 1.631$$

and thus

$$\mu/\lambda = -3.033 \quad R/\lambda = 1.379 \quad E_1/\lambda = -2.214$$

The magnetic moment of  $\text{Fe}(\text{diammac})^{3+}$  at 295 K was determined by the Evans method.<sup>13</sup> A value of  $\mu_{\text{eff}}$  of 2.20  $\mu_B$  was found, which is higher than the spin-only value (1.73  $\mu_B$ ), indicative of a significant orbital contribution to the magnetic moment. The effect of axial distortion on the behavior of  $\mu_{\text{eff}}$  as a function of  $kT/|\lambda|$  has been discussed.<sup>28</sup> A reasonable estimate of  $\lambda$  may be extracted from a plot of  $\mu_{\text{eff}}$  versus  $kT/|\lambda|$ , where the axial distortion parameter  $\mu/\lambda = -3.033$ , yielding an approximate value of  $\lambda = -310 \text{ cm}^{-1}$ , comparable with values for other low-spin (hexaamine)iron(III) complexes.<sup>27</sup> The estimated value of  $\lambda$  allows absolute values of  $\mu$ ,  $R$ , and  $E_1$  to be calculated, although the

(21) Comba, P.; Horn, E.; Sargeson, A. M.; Snow, M. R. Unpublished work.

(22) Geilenkirchen, A.; Wieghardt, K.; Nuber, B.; Weiss, J. *Z. Naturforsch.* **1989**, *44B*, 1333.

(23) Marsh, R. E. *Acta Crystallogr. Sect. B* **1987**, *B34*, 174.

(24) Curtis, N. F.; Gainsford, G. J.; Hambley, T. W.; Lawrence, G. A.; Morgan, K. R.; Siriwardena, A. *J. Chem. Soc., Chem. Commun.* **1987**, 295.

(25) Hambley, T. W. *Inorg. Chem.* **1988**, *27*, 2496.

(26) McGarvey, B. R. *Transition Metal Chem.* **1966**, *3*, 89.

(27) Bohan, T. L. *J. Magn. Reson.* **1977**, *26*, 109.

(28) Figgis, B. N. *Introduction to Ligand Fields*; Wiley: New York, 1966.

**Table VI.** Interelectron Repulsion Parameters, Ligand Field Splitting Energies, and Spectrochemical Ligand Parameters ( $f$ ) for  $M(\text{diammac})^{n+}$  Complexes

$M^{n+}$	$B, \text{cm}^{-1}$	$C, \text{cm}^{-1}$	$Dq, \text{cm}^{-1}$	$f$	ref
$\text{Cr}^{3+}$	620	3301	2342	1.35	9
$\text{Co}^{3+}$	575	4243	2562	1.35	7
$\text{Rh}^{3+}$	409		3624	1.34	10
$\text{Ni}^{2+}$	980		1256	1.44	35
$\text{Fe}^{3+}$	614	2656	2234	1.60 <sup>a</sup>	this work

<sup>a</sup> 1.37 for reassessed value of  $g = 16.3 \text{ cm}^{-1}$ .

uncertainties introduced by the approximate value of  $\lambda$  must be taken into consideration.

The electronic spectrum of  $[\text{Fe}(\text{diammac})]^{3+}$  was also indicative of a low-spin  $d^5$  configuration in an octahedral ligand field ( ${}^2T_{2g}$  ground state). Five maxima were discernible:  $8645 \text{ cm}^{-1}$  ( $\epsilon 0.01 \text{ M}^{-1} \text{ cm}^{-1}$ ) ( ${}^4T_{1g} \leftarrow {}^2T_{2g}$ );  $17857$  (broad,  $\epsilon 1$ ) ( ${}^2A_{2g} \leftarrow {}^2T_{2g}$ );  $20833$  (shoulder,  $\epsilon 30$ ) ( ${}^2T_{2g} \leftarrow {}^2T_{2g}$ );  $23981$  ( $\epsilon 55$ ) ( ${}^2E_g \leftarrow {}^2T_{2g}$ );  $30120$  ( $\epsilon 140$ ) ( ${}^2A_{1g} \leftarrow {}^2T_{2g}$ );  $33898$  (shoulder,  $\epsilon 235$ ). The last transition is not assignable to a d-d transition. It is appropriate at this stage to quantify the strength of the ligand field imposed by diammac, since there now exist six metal complexes where the ligand acts in a sixdentate fashion and five that yield an electronic spectrum ( $\text{Zn}(\text{diammac})^{2+}$  being the exception). Table VI shows a list of calculated<sup>29</sup> Racah parameters  $B$  and  $C$  (not to be confused with the coefficients  $A$ ,  $B$ , and  $C$  in the EPR analysis), ligand field splitting energies,  $Dq$ , and the ligand spectrochemical parameter,  $f$ , where

$$100fg = Dq$$

and where  $g$  is the empirical spectrochemical parameter for the metal ion in question (unrelated to the  $g$  values in the EPR spectrum). The rather high value of  $f$  determined from the spectrum of  $[\text{Fe}(\text{diammac})]^{3+}$  is not in agreement with the values determined from the other spectra. Since a reasonable calculation of  $f$  is dependent on  $g$ , the discrepancy between the determined  $f$  values from the  $[\text{Fe}(\text{diammac})]^{3+}$  spectrum and those calculated from the other spectra seems to indicate that the empirical spectrochemical parameter for iron(III) ( $14.0 \text{ cm}^{-1}$ )<sup>30</sup> is lower than it should be; a more reasonable value, using the average value of  $f_{\text{diammac}} = 1.37$ , is  $g_{\text{Fe(III)}} = 16.3 \text{ cm}^{-1}$ . This adjustment is justifiable when one considers that there have been few analyses of the electronic spectra of a series of complexes, where the series has included low-spin iron(III), with identical ligand fields. Nevertheless, the value of  $f_{\text{diammac}} = 1.37$  places the ligand high in the spectrochemical series, just above 2,2'-bipyridyl. It should be pointed out that ligands in the series with higher  $f$  values than

diammac all form metal-ligand bonds with a large degree of  $\pi$  character, e.g.  $\text{CN}^-$  and  $\text{NO}_2^-$ , which results in these ligands possessing extremely large  $f$  values. Therefore, diammac is the strongest purely  $\sigma$ -bonding ligand reported, so far, in the literature.

When all of the physical and structural data are considered, two factors seem relevant to explain the unusual stability of  $[\text{Fe}(\text{diammac})]^{3+}$  in aerated aqueous solution. First, one of the more common reactions that occur with iron(III) amine complexes is oxidative dehydrogenation of the ligand to form coordinated imines with concomitant reduction of the metal center to the divalent state.<sup>31-34</sup> Clearly, the more negative the  $\text{Fe}^{\text{III/II}}$  redox couple, the less likely oxidative dehydrogenation becomes, and the relatively negative half-wave potential of  $-0.35 \text{ V}$  vs  $\text{Ag}/\text{AgCl}$  for  $[\text{Fe}(\text{diammac})]^{3+}$  acts to stabilize the complex. Second, the structure of  $[\text{Fe}(\text{diammac})]^{3+}$  reveals a rather rigid and, more importantly, nonplanar, conformation of the macrocycle. To change the coordinated nitrogens donors from amines to imines (tetrahedral to trigonal-planar geometry) would introduce considerable strain in the ligand, and dissociation of the complex would almost certainly occur. Another important factor contributing to the stability of the complex is the absence of hydrogens in  $\alpha$ -positions to the pendant amines, which necessarily disallows dehydrogenation in these positions.

### Conclusion

The stability of  $[\text{Fe}(\text{diammac})]^{3+}$  in aerated aqueous solution has provided a rare opportunity to study a low-spin (hexamine)-iron(III) complex without the hazards of ligand dehydrogenation and complex dissociation. The short Fe-N bond lengths that result from coordination of the strong field pendant-arm macrocycle act to stabilize the metal center in its trivalent state. The analyses of the EPR and electronic spectra of  $[\text{Fe}(\text{diammac})]^{3+}$  were simplified to a great degree by the absence of  $\pi$  bonding between the metal ion and the nitrogen donors, a factor that has, in the past, clouded the spectroscopy of low-spin iron(III) complexes through electron delocalization and charge-transfer electronic transitions.

**Acknowledgment.** Support of the Australian Research Council and the Swiss National Science Foundation (Grant No. 20-5597.88) is gratefully acknowledged.

**Supplementary Material Available:** Tables of crystal data, non-hydrogen thermal parameters, hydrogen atom positional and thermal parameters, and close intermolecular contacts (3 pages); a listing of observed and calculated structure factors (10 pages). Ordering information is given on any current masthead page.

(29) Lever, A. B. P. *Inorganic Electronic Spectroscopy*; Elsevier: New York, 1968.  
 (30) Jørgenson, C. K. *Absorption Spectra and Chemical Bonding*; Pergamon Press: Oxford, England, 1962.

(31) Dabrowiak, J. C.; Lovecchio, F. V.; Goedken, V. L.; Busch, D. H. *J. Am. Chem. Soc.* **1972**, *94*, 5502.  
 (32) Dabrowiak, J. C.; Busch, D. H. *Inorg. Chem.* **1975**, *14*, 1881.  
 (33) Goto, M.; Takeshita, M.; Kanda, N.; Sakai, T.; Goedken, V. L. *Inorg. Chem.* **1985**, *24*, 582.  
 (34) Kuroda, Y.; Tanaka, N.; Goto, M.; Sakai, T. *Inorg. Chem.* **1989**, *28*, 2163.  
 (35) Siriwardena, A. Doctoral Dissertation, Victoria University of Wellington, New Zealand, 1989.